



Will an imperfect vaccine curtail the COVID-19 pandemic in the U.S.?



Enahoro A. Iboi ^d, Calistus N. Ngonghala ^b, Abba B. Gumel ^{a, c, *}

^a School of Mathematical and Statistical Sciences, Arizona State University, Tempe, AZ, 85287, USA

^b Department of Mathematics, University of Florida, Gainesville, FL, 32611, USA

^c Department of Mathematics and Applied Mathematics, University of Pretoria, Pretoria, 0002, South Africa

^d Department of Mathematics, Spelman College, Atlanta, Georgia, 30314, USA

ARTICLE INFO

Article history:

Received 9 May 2020

Received in revised form 29 June 2020

Accepted 24 July 2020

Available online 6 August 2020

Handling Editor: Dr. J Wu

Keywords:

COVID-19

SARS-CoV-2

Vaccination

Social distancing

Non-pharmaceutical intervention

ABSTRACT

The novel coronavirus (COVID-19) that emerged from Wuhan city of China in late December 2019 continue to pose devastating public health and economic challenges across the world. Although the community-wide implementation of basic non-pharmaceutical intervention measures, such as social distancing, quarantine of suspected COVID-19 cases, isolation of confirmed cases, use of face masks in public, contact tracing and testing, have been quite effective in curtailing and mitigating the burden of the pandemic, it is universally believed that the use of a vaccine may be necessary to effectively curtail and eliminating COVID-19 in human populations. This study is based on the use of a mathematical model for assessing the impact of a hypothetical imperfect anti-COVID-19 vaccine on the control of COVID-19 in the United States. An analytical expression for the minimum percentage of unvaccinated susceptible individuals needed to be vaccinated in order to achieve vaccine-induced community herd immunity is derived. The epidemiological consequence of the herd immunity threshold is that the disease can be effectively controlled or eliminated if the minimum herd immunity threshold is achieved in the community. Simulations of the model, using baseline parameter values obtained from fitting the model with COVID-19 mortality data for the U.S., show that, for an anti-COVID-19 vaccine with an assumed protective efficacy of 80%, at least 82% of the susceptible US population need to be vaccinated to achieve the herd immunity threshold. The prospect of COVID-19 elimination in the US, using the hypothetical vaccine, is greatly enhanced if the vaccination program is combined with other interventions, such as face mask usage and/or social distancing. Such combination of strategies significantly reduces the level of the vaccine-induced herd immunity threshold needed to eliminate the pandemic in the US. For instance, the herd immunity threshold decreases to 72% if half of the US population regularly wears face masks in public (the threshold decreases to 46% if everyone wears a face mask).

© 2020 The Authors. Production and hosting by Elsevier B.V. on behalf of KeAi Communications Co., Ltd. This is an open access article under the CC BY-NC-ND license (<http://creativecommons.org/licenses/by-nc-nd/4.0/>).

* Corresponding author. School of Mathematical and Statistical Sciences, Arizona State University, Tempe, AZ, 85287, USA.

E-mail address: agumel@asu.edu (A.B. Gumel).

Peer review under responsibility of KeAi Communications Co., Ltd.

1. Introduction

In December 2019, the Wuhan Municipal Health Commission, China, reported a cluster of a pneumonia-like illness, caused by a coronavirus (SARS-CoV-2) in Wuhan, Hubei Province of China (Li et al., 2020; World Health Organization, 2020a; World Health Organization). The disease rapidly spread to many countries, resulting in the World Health Organization declaring the novel coronavirus (COVID-19) as a pandemic on March 11, 2020 (Ngonghala et al., 2020; World Health Organization, 2020a; World Health Organization). As of June 28, 2020, COVID-19 has caused over 10 million confirmed cases and 500,000 fatalities globally. The United States, which is now the epicenter of COVID-19, recorded over 2.5 million confirmed cases and 125,000 deaths (“Center for Systems Scien, 2020). While some people infected with COVID-19 experience mild symptoms of the disease (such as fever, coughing and shortness of breath), others develop severe disease and complications (causing acute respiratory failure, which damages the lungs and often cause death) (Knvul and Katie, 2020; Ngonghala et al., 2020; World Health Organization, 2020b). In addition to the devastating public health burden it induced in the US, COVID-19 has also inflicted severe economic hardship, causing a decrease in both human and economic productivity (translating to about 30% unemployment rate, and a projected 50% decline in GDP by the summer of 2020 (Matthews, 2020; Rotman, 2020)).

There are currently no approved vaccines and effective therapies for use against COVID-19. Hence, control efforts against COVID-19 are focused on using basic non-pharmaceutical interventions (NPIs), such as social distancing, quarantine of people suspected of being exposed to COVID-19, isolation of confirmed cases, use of face masks in public and contact-tracing (Ngonghala et al., 2020; Ferguson et al., 2020; Eikenberry et al., 2020). There is now a concerted global effort to develop a safe and effective anti-COVID-19 vaccine to help combat the COVID-19 pandemic. Although the development of new vaccines generally take years, a number of pharmaceutical companies, with support from numerous government agencies and regulatory authorities, are doing everything possible to fast-track the availability of a safe and effective vaccine against COVID-19. Over a dozen organizations have announced plans to start efficacy testing for their candidate vaccines (Knvul and Katie, 2020; Callaway, 2020; Kirkpatrick, 2020). In fact, scientists at the Jenner Institute at the Oxford University have developed a new coronavirus vaccine that is undergoing early-phase trials, and they expect the first few million doses of their vaccine to be widely available as early as September 2020 (Callaway, 2020; Kirkpatrick, 2020). A Maryland-based biotechnology company Novavax has begun human clinical trials for its candidate vaccine in Australia (Knvul and Katie, 2020). Similarly, Mesoblast, a company supported by the National Institutes of Health (NIH), started a 240-patient clinical trial aimed at testing whether cells derived from bone marrow could help patients who developed a deadly immune reaction to the coronavirus (Knvul and Katie, 2020). Thus, there is an urgent need to develop and use mathematical models to assess the population-level impact of a future hypothetical vaccine against COVID-19. This forms the objective of the current study.

Numerous mathematical models have been developed and used to study the transmission dynamics and control of COVID-19. For instance, an agent-based model was developed by Ferguson et al. (Ferguson et al., 2020) to investigate the impact of NPIs on COVID-19-induced mortality, showing an alarming worst-case projection of number of cases for the US and Great Britain (at the tune of 81%). Eikenberry et al. (Eikenberry et al., 2020) developed a multi-group model for assessing the community-wide impact of mask use by the general, asymptomatic public, a portion of which may be asymptotically-infectious. The study shows that the use of face masks by members of the general public is potentially of high value in curtailing community transmission and the burden of the pandemic, and that the community-wide benefits are likely to be greatest when face masks are used in conjunction with other non-pharmaceutical practices (such as social distancing), and when adoption is nearly universal (nation-wide) and compliance is high. Ngonghala et al. (Ngonghala et al., 2020) developed a comprehensive model for assessing the impact of the major NPIs (quarantine, isolation, social distancing, face mask usage in public, testing and contact-tracing) on the control of COVID-19. Their study estimated that, while the early relaxation or lifting social distancing measures and mask usage is likely to lead to second wave, the extended adherence to the current social distancing and mask usage can significantly reduce COVID-induced mortality in the US in general, and the state of New York in particular.

Mizumoto and Chowell (Mizumoto & Chowell, 2020) modeled the potential for a COVID-19 outbreak in the Diamond Princess cruise ship. Their study showed an estimate of a higher reproduction number, which substantially decreases with increasing effectiveness of quarantine measures on the ship. A stochastic model was developed by Hellewell et al. (Hellewell et al., 2020) to assess the impact of contact-tracing and isolation on disease control. Their study suggests that (for most instances) the spread of COVID-19 can be effectively contained in 3 months if the two control measures (contact-tracing and isolation) are highly effective. Kucharski et al. (Kucharski et al., 2020) also developed a stochastic model to assess the COVID-19 trajectory in Wuhan from January to February 2020, showing a reduction in transmission when travel restrictions were implemented. Li et al. developed a mathematical model to assess the effect of mass influenza vaccination on the spread of COVID-19 and other influenza-like pathogens co-circulating during an influenza season. Their study showed that increasing influenza vaccine uptake, or enhancing the public health interventions, would facilitate the management of outbreaks of respiratory pathogens circulating during the peak flu season.

The current study is based on the design of a mathematical model to assess the impact of an anti-COVID-19 vaccine on the transmission dynamics of the COVID-19 pandemic in the United States. COVID-19 mortality data for the US will be used to fit the model, and to estimate the unknown parameters of the model (notably the contact rate parameters).

2. Materials and methods

2.1. Model formulation

This study is based on the development of a relatively standard mathematical model for assessing the population-level impact of a potential hypothetical anti-COVID-19 vaccine in a community. The model is developed by splitting the total human population at time t , denoted by $N(t)$, into the mutually-exclusive compartments of unvaccinated susceptible ($S_u(t)$), vaccinated susceptible ($S_v(t)$), early-exposed ($E_1(t)$; i.e., newly-exposed individuals), pre-symptomatic infectious ($E_2(t)$), symptomatically-infectious ($I_s(t)$), asymptotically-infectious ($I_a(t)$), hospitalized ($I_h(t)$) and recovered ($R(t)$) individuals. Thus,

$$N(t) = S_u(t) + S_v(t) + E_1(t) + E_2(t) + I_s(t) + I_a(t) + I_h(t) + R(t).$$

It should be emphasized that individuals in the E_2 compartment are those newly-infected individuals that are close to surviving the incubation period, and are shedding the virus. Hence, they are infectious (i.e., they are able to transmit COVID-19 infection to susceptible individuals). Furthermore, while individuals in the I_s are those that show moderate to severe symptoms of COVID-19 at the end of the incubation period, those in the I_a compartment are assumed to show mild or no clinical symptoms of the disease at the end of the incubation period. The compartment I_h also contains individuals with clinical symptoms of COVID-19 who are hospitalized or self-isolated at home.

The model is given by the following deterministic system of nonlinear differential equations, where a dot represents differentiation with respect to time t (a flow diagram of the model is depicted in Fig. 1. The state variables and parameters of the model are described in Tables 1 and 2, respectively):

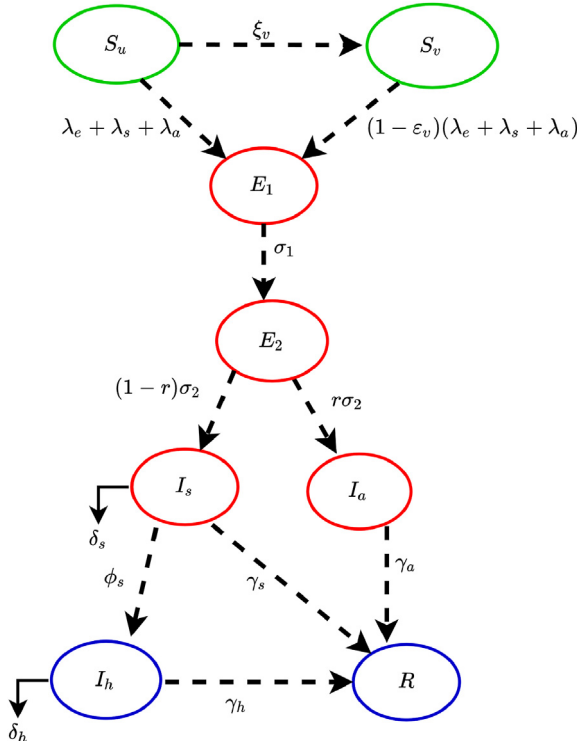


Fig. 1. Flow diagram of the model (2.1).

Table 1

Description of state variables of the model (2.1).

State variable	Description
S_u	Population of unvaccinated susceptible individuals
S_v	Population of vaccinated susceptible individuals
E_1	Population of early-exposed individuals (i.e., newly-infected individuals who are not yet infectious)
E_2	Population of pre-symptomatic infectious individuals (i.e., exposed individuals who are close to surviving the incubation period and are shedding virus)
I_s	Population of symptomatically-infectious individuals (who display moderate or severe symptoms of the disease at the end of the incubation period)
I_a	Population of asymptotically-infectious individuals (who display mild or no clinical symptoms of the disease at the end of the incubation period)
I_h	Population of hospitalized individuals
R	Population of recovered individuals

Table 2

Description of the parameters of the model (2.1).

Parameter	Description
$\beta_e(\beta_s)(\beta_a)$	Effective community contact rate (a measure of social distancing effectiveness)
c_M	Proportion of members of public who wear masks in public (i.e., face masks compliance)
ε_M	Efficacy of face masks to prevent acquisition of infection by susceptible individuals
ξ_v	Vaccination rate
ε_v	Vaccine efficacy against acquisition of infection (degree protection)
r	Proportion of pre-symptomatic individuals who do not show clinical symptoms of COVID-19 at the end of the incubation period
$1 - r$	Proportion of pre-symptomatic infectious individuals who show clinical symptoms of COVID-19 at the end of the incubation period
σ_1	Rate of progression from early-exposed class (E_1) to the pre-symptomatic class
$r\sigma_2$	Rate of progression from pre-symptomatic class (E_2) to asymptotically-infectious class
$(1 - r)\sigma_2$	Rate of progression from pre-symptomatic class (E_2) to symptomatically-infectious class
φ_s	Hospitalization rate for infectious individuals
$\gamma_s(\gamma_a)(\gamma_h)$	Recovery rate for individuals in the $I_s(I_a)(I_h)$ class
$\delta_s(\delta_h)$	Disease-induced mortality rate for infectious individuals in the $I_s(I_h)$ class

$$\begin{aligned}
 \dot{S}_u &= -(\lambda_e + \lambda_s + \lambda_a)S_u - \xi_v S_u, \\
 \dot{S}_v &= \xi_v S_u - (1 - \varepsilon_v)(\lambda_e + \lambda_s + \lambda_a)S_v, \\
 \dot{E}_1 &= (\lambda_e + \lambda_s + \lambda_a)[S_u + (1 - \varepsilon_v)S_v] - \sigma_1 E_1, \\
 \dot{E}_2 &= \sigma_1 E_1 - \sigma_2 E_2, \\
 \dot{I}_s &= (1 - r) \sigma_2 E_2 - (\varphi_s + \gamma_s + \delta_s)I_s, \\
 \dot{I}_a &= r \sigma_2 E_2 - \gamma_a I_a, \\
 \dot{I}_h &= \varphi_s I_s - (\gamma_h + \delta_h)I_h, \\
 \dot{R} &= \gamma_s I_s + \gamma_a I_a + \gamma_h I_h,
 \end{aligned} \tag{2.1}$$

where the forces of infection λ_e , λ_s and λ_a are defined below

$$\lambda_e = \beta_e(1 - \varepsilon_M c_M) \frac{E_2}{N}, \quad \lambda_s = \beta_s(1 - \varepsilon_M c_M) \frac{I_s}{N}, \quad \lambda_a = \beta_a(1 - \varepsilon_M c_M) \frac{I_a}{N}. \tag{2.2}$$

In the model (2.1), unvaccinated susceptible individuals acquire COVID-19 infection, following effective contacts with individuals in the E_2 , I_a and I_s classes, at the rates λ_e , λ_s and λ_a , respectively. Unvaccinated susceptible individuals are vaccinated at a *per capita* rate ξ_v . It is assumed that the hypothetical anti-COVID-19 vaccine is imperfect. Hence, the vaccine allows for breakthrough infected in vaccinated susceptible individuals who became infected with COVID-19, with a protective efficacy $0 < \varepsilon_v \leq 1$ (i.e., vaccinated susceptible individuals are assumed to acquire COVID-19 infection, following effective contact with individuals in the E_2 , I_s and I_a classes at the reduced rates, $(1 - \varepsilon_v)\lambda_e$, $(1 - \varepsilon_v)\lambda_s$ and $(1 - \varepsilon_v)\lambda_a$, respectively).

The parameter σ_1 represents the progression rate of individuals in the early-exposed class (i.e., individuals in the E_1 class) to the pre-symptomatic infectious class (E_2). Similarly, σ_2 is the rate at which pre-symptomatic individuals progress, at the end of the incubation period, to either the asymptotically-infectious class, I_a (at a rate $r\sigma_2$; where $0 < r \leq 1$ is the proportion of pre-symptomatic infectious individuals who do not show clinical symptoms of COVID-19 at the end of the incubation period) or to the symptomatically-infectious class, I_s (at a rate $(1 - r)\sigma_2$). Thus, the intrinsic incubation period of COVID-19 is given by $\frac{1}{\sigma_1} + \frac{1}{\sigma_2}$. The parameter $\gamma_s(\gamma_a)(\gamma_h)$ represents the recovery rate for individuals in the $I_s(I_a)(I_h)$ class. Similarly, φ_s is the hospitalization (or self-isolation) rate of individuals with clinical symptoms of COVID-19. Finally, the parameter $\delta_s(\delta_h)$ represents the COVID-induced mortality rate for individuals in the $I_s(I_h)$ class. It should be mentioned that,

since not much data is available on the expected properties of a future anti-COVID-19 vaccine, we do not assume that the vaccine offers any therapeutic benefits. Further, we do not assume that the vaccine wanes during the one-year time period we would choose for the numerical simulations of our model.

In (2.2), the parameter $\beta_e(\beta_s)(\beta_a)$ represents the effective contact rate (i.e., contacts capable of leading to COVID-19 transmission) for pre-symptomatically-infectious (symptomatically-infectious) (asymptomatically-infectious) individuals, $0 < c_M \leq 1$ is the proportion of members of the public who wear face masks (correctly and consistently) in public and $0 < \varepsilon_M \leq 1$ is the efficacy of the face masks. This formulation (i.e., $\beta_e \neq \beta_s \neq \beta_a$) allows us to account for the possible heterogeneity in the contact rates of infectious individuals in the pre-symptomatic (E_2), symptomatic (I_s) and asymptomatic (I_a) classes. The basic model (2.1) may be the first to explicitly incorporates a hypothetical imperfect vaccine in a deterministic modeling study on COVID-19 dynamics.

It is convenient, for housekeeping purposes, to define the following equation for the rate of change of the population of COVID-deceased individuals in the community (denoted by $D(t)$):

$$\dot{D} = \delta_s I_s + \delta_h I_h. \quad (2.3)$$

3. Theoretical analysis

3.1. Asymptotic stability of disease-free equilibria

The model (2.1) has a continuum (or line) of disease-free equilibria (DFE), given by

$$\mathcal{E}_0 : (S_u^*, S_v^*, E_1^*, E_2^*, I_s^*, I_a^*, I_h^*, R^*) = (N(0) - (S_v^* + R^*), S_v^*, 0, 0, 0, 0, 0, R^*),$$

where $N(0)$ is the initial total population size, $S_v^* > 0, R^* > 0$, and $0 \leq S_v^* + R^* \leq N(0) = N^*$. The next generation operator method (van den Driessche & Watmough, 2002; Diekmann et al., 1990) can be used to analyse the asymptotic stability property of the continuum of disease-free equilibria, \mathcal{E}_0 . In particular, using the notation in (van den Driessche & Watmough, 2002), it follows that the associated next generation matrices, F and V , for the new infection terms and the transition terms, are given, respectively, by

$$F = \begin{bmatrix} 0 & A_e & A_s & A_a \\ 0 & 0 & 0 & 0 \\ 0 & 0 & 0 & 0 \\ 0 & 0 & 0 & 0 \end{bmatrix},$$

and,

$$V = \begin{bmatrix} \sigma_1 & 0 & 0 & 0 \\ -\sigma_1 & \sigma_2 & 0 & 0 \\ 0 & -(1-r)\sigma_2 & \varphi_s + \gamma_s + \delta_s & 0 \\ 0 & -r\sigma_2 & 0 & \gamma_a \end{bmatrix},$$

where,

$$\begin{aligned} A_e &= \beta_e(1 - \varepsilon_M c_M) \left[\frac{S_u^* + (1 - \varepsilon_v)S_v^*}{N^*} \right], \\ A_s &= \beta_s(1 - \varepsilon_M c_M) \left[\frac{S_u^* + (1 - \varepsilon_v)S_v^*}{N^*} \right], \\ A_a &= \beta_a(1 - \varepsilon_M c_M) \left[\frac{S_u^* + (1 - \varepsilon_v)S_v^*}{N^*} \right]. \end{aligned}$$

It is convenient to define the quantity \mathcal{R}_c by (with ρ being the spectral radius):

$$\mathcal{R}_c = \rho(FV^{-1}) = \mathcal{R}_{E_2} + \mathcal{R}_{I_s} + \mathcal{R}_{I_a}, \quad (3.1)$$

where,

$$\begin{aligned}
\mathcal{R}_{E_2} &= \frac{\beta_e(1 - \varepsilon_M c_M)}{\sigma_2} \left[\frac{S_u^* + (1 - \varepsilon_v)S_v^*}{N^*} \right], \\
\mathcal{R}_{I_s} &= \frac{\beta_s(1 - r)(1 - \varepsilon_M c_M)}{\phi_s + \gamma_s + \delta_s} \left[\frac{S_u^* + (1 - \varepsilon_v)S_v^*}{N^*} \right], \\
\mathcal{R}_{I_a} &= \frac{\beta_a r(1 - \varepsilon_M c_M)}{\gamma_a} \left[\frac{S_u^* + (1 - \varepsilon_v)S_v^*}{N^*} \right].
\end{aligned} \tag{3.2}$$

The quantity \mathcal{R}_c is the *control reproduction number* of the model (2.1). It measures the average number of new COVID-19 cases generated by a typical infectious individual introduced into a population where a certain fraction wears face masks in public and/or are vaccinated using the hypothetical imperfect vaccine. It is the sum of the constituent reproduction numbers associated with the number of new cases generated by pre-symptomatically-infectious humans (\mathcal{R}_{E_2}), symptomatically-infectious humans (\mathcal{R}_{I_s}), and asymptomatically-infectious (\mathcal{R}_{I_a}) individuals. The reproduction number \mathcal{R}_c is epidemiologically interpreted below.

3.1.1. Interpretation of the control reproduction number

As stated above, the control reproduction number \mathcal{R}_c is the sum of the three constituent reproduction numbers, \mathcal{R}_{E_2} , \mathcal{R}_{I_s} , and \mathcal{R}_{I_a} . The constituent reproduction number \mathcal{R}_{E_2} is given by the product of the infection rate of unvaccinated and vaccinated susceptible individuals by pre-symptomatically-infectious humans (near the continuum of disease-free equilibria), $\left[\beta_e(1 - \varepsilon_M c_M) \left(\frac{S_u^* + (1 - \varepsilon_v)S_v^*}{N^*} \right) \right]$, the proportion of exposed individuals that survived the pre-exposed period and moved to the pre-symptomatically-infectious class and the average duration in the pre-symptomatically-infectious class $\left(\frac{1}{\sigma_2} \right)$. Similarly, the constituent reproduction number \mathcal{R}_{I_s} is given by the product of the infection rate of unvaccinated and vaccinated susceptible individuals by symptomatically-infectious humans (near the continuum of disease-free equilibria), $\left[\beta_s(1 - \varepsilon_M c_M) \left(\frac{S_u^* + (1 - \varepsilon_v)S_v^*}{N^*} \right) \right]$, the proportion of exposed individuals that survived the incubation period and moved to the symptomatically-infectious class $\left(\frac{(1-r)\sigma_2}{\sigma_2} = 1 - r \right)$ and the average duration in the asymptomatically-infectious class $\left(\frac{1}{\phi_s + \gamma_s + \delta_s} \right)$. Finally, the constituent reproduction number \mathcal{R}_{I_a} is given by the product of the infection rate of unvaccinated and vaccinated susceptible individuals (near the continuum of disease-free equilibria), $\left[\beta_a(1 - \varepsilon_M c_M) \left(\frac{S_u^* + (1 - \varepsilon_v)S_v^*}{N^*} \right) \right]$, the proportion that survived the exposed class and moved to the asymptomatically-infectious class $\left(\frac{r\sigma_2}{\sigma_2} = r \right)$ and the average duration in the I_a class $\left(\frac{1}{\gamma_a} \right)$. The sum of \mathcal{R}_{E_2} , \mathcal{R}_{I_s} , and \mathcal{R}_{I_a} gives \mathcal{R}_c .

The result below follows from the next generation matrix operator method of (van den Driessche & Watmough, 2002).

Theorem 3.1. *The continuum of disease-free equilibria (\mathcal{E}_0) of the model (2.1) is locally-asymptotically stable if $\mathcal{R}_c < 1$. If $\mathcal{R}_c > 1$, the epidemic first grows, reaches a peak, and then decreases to zero as $t \rightarrow \infty$.*

The epidemiological implication of Theorem 3.1 is that a small influx of COVID-19 cases will not generate a COVID-19 outbreak if the control reproduction number (\mathcal{R}_c) is less than unity (i.e., the epidemic dies out rapidly whenever $\mathcal{R}_c < 1$). It should be mentioned that, for epidemic models such as (2.1), the epidemiological requirement $\mathcal{R}_c < 1$ is only sufficient, but not necessary, for the elimination of the epidemic. This is owing to the fact that, for such models (i.e., Kermack-McKendrick epidemic models with no vital/demographic dynamics), the disease always dies out with time (regardless of the value of the reproduction number of the models). In other words, even if \mathcal{R}_c exceeds unity, the disease will eventually die out. This is because (if $\mathcal{R}_c > 1$), the epidemic rises (exponentially, initially) and reach a peak. Subsequently, a combination of factors, such as the implementation of control measures in the community and the natural infection-acquired immunity in the community, will greatly curtail the epidemic to the extent that sustained community transmission is not feasible (and the disease dies out) (Nishiura & Chowell, 2009). It is worth stressing that, in the formulation of the model (2.1), we assumed that individuals who survived the COVID-19 infection develop permanent natural immunity against future COVID-19 infection (since there is no transition from the recovered to the susceptible class in the model). This natural immunity builds up in the community and contributes in protecting the rest of the susceptible population from acquiring COVID-19 infection. If recruitment of susceptible individuals is allowed (e.g., in the case where an endemic model is used), the disease will persist in the population when $\mathcal{R}_c > 1$ (this is because the pool of new completely-susceptible, or COVID-19-naive, individuals will continuously be replenished, by birth or immigration, thereby allowing the disease to sustain itself in the community).

It is convenient to define the following feasible (positively-invariant and attracting) region for the model (2.1)

$$\Omega = \left\{ (S_u, S_v, E_1, E_2, I_s, I_a, I_h, R) \in \mathbb{R}_+^8 : S_u + S_v + E_1 + E_2 + I_s + I_a + I_h + R \leq N(0) \right\}.$$

We claim the following result:

Theorem 3.2. *The continuum disease-free equilibria (\mathcal{E}_0) of the model (2.1) is globally-asymptotically stable in Ω if $\mathcal{R}_c \leq 1$.*

The Proof to Theorem 3.2, based on using Lyapunov function theory, is given in [Appendix A](#). Here, too, the requirement $\mathcal{R}_c \leq 1$ is sufficient, and not necessary, for the elimination of the pandemic. The epidemiological implication of this result is that COVID-19 elimination is independent of the initial sizes of the sub-populations of the model (i.e., the initial number of infected individuals introduced into the community does not have to be within the basin of attraction of the continuum of the disease-free equilibria, \mathcal{E}_0 of the model).

In the absence of control interventions (i.e., no face mask usage and vaccination) in the community vaccination, the control reproduction number (\mathcal{R}_c) (3.1) reduces to the basic reproduction number (denoted by \mathcal{R}_0), given by:

$$\mathcal{R}_0 = \mathcal{R}_c|_{c_M = \epsilon_M = \epsilon_v = S_v^* = 0} = \frac{\beta_e}{\sigma_2} + \frac{(1 - r)\beta_s}{\varphi_s + \gamma_s + \delta_s} + \frac{r\beta_a}{\gamma_a} \quad (3.3)$$

The quantity \mathcal{R}_0 represents the average number of new infections generated by a typical COVID-19 infected individual introduced into a completely susceptible population during the duration of his/her infectiousness. It is convenient to define the following quantity

$$\mathcal{R}_0^* = \mathcal{R}_c|_{c_M = \epsilon_M = 0} = \mathcal{R}_0 \left[\frac{S_u^* + (1 - \epsilon_v)S_v^*}{N^*} \right], \quad (3.4)$$

which represents the control reproduction number of the model in the absence of face masks usage in the community.

3.2. Model fitting and parameter estimation

Some of the parameters of the model (2.1) were obtained either from the literature, or assumed based on publicly-available COVID-19 related information ([Table 3\(a\)](#)). For the six parameters whose numerical values are not known, namely the community contact rates (β_e , β_a and β_s), the hospitalization rate of symptomatic individuals (φ_s), mask compliance (c_M), and the COVID-19-related mortality rate of hospitalized individuals (δ_h), we estimated them using the COVID-19 mortality data for the US from March 1, 2020 to June 23, 2020 ([Centers for Disease Control and Prevention, 2019](#); [Dong, Du, & Gardner, 2020a](#), [Dong, Du, & Gardner, 2020](#); [Dong et al., 2020a](#), [Dong, Du, & Gardner, 2020](#); [World Health Organization, 2019](#)). Although the first documented COVID-19 case in the US was reported January 20, 2020 ([Holshue et al., 2020](#)), there were less than 30 confirmed cases in the US by March 1, 2020 ([Dong et al., 2020a](#), [Dong, Du, & Gardner, 2020](#)). Hence, we used data from March 1 onward in estimating our parameters, and we also start all our simulations from March 1. Also, since the mortality data was collected when no vaccination program is in place, we fitted these parameters to the special case of the model (2.1) without vaccination. To

Table 3

Parameters of the model (2.1).

(a) Parameter values from the literature (and those assumed)		
Parameter	Default values	Reference
ϵ_M	0.5 (dimensionless)	Estimated from (Davies et al., 2013)
ϵ_v	0.8 (dimensionless)	Assumed
ξ_v	0.0203 day ⁻¹	Assumed
σ_1	1/4 day ⁻¹	Adapted from (Center for Disease Control and Prevention, n.d.)
σ_2	1/2 day ⁻¹	Adapted from (Center for Disease Control and Prevention, n.d.)
R	0.35	
γ_a	1/7 day ⁻¹	(Tang et al., 2020 ; Zhou et al., 2020)
γ_s	1/7 day ⁻¹	(Tang et al., 2020 ; Zhou et al., 2020)
γ_h	1/14 day ⁻¹	(Tang et al., 2020 ; Zhou et al., 2020)
δ_s	$\delta_h/3$ day ⁻¹	Estimated

(b) Fitted parameters	
Parameter	Fitted value
β_e	0.1004 day ⁻¹
β_a	0.7701 day ⁻¹
β_s	0.3214 day ⁻¹
φ_s	0.0514 day ⁻¹
c_M	0.1704 (dimensionless)
δ_h	0.0001 day ⁻¹

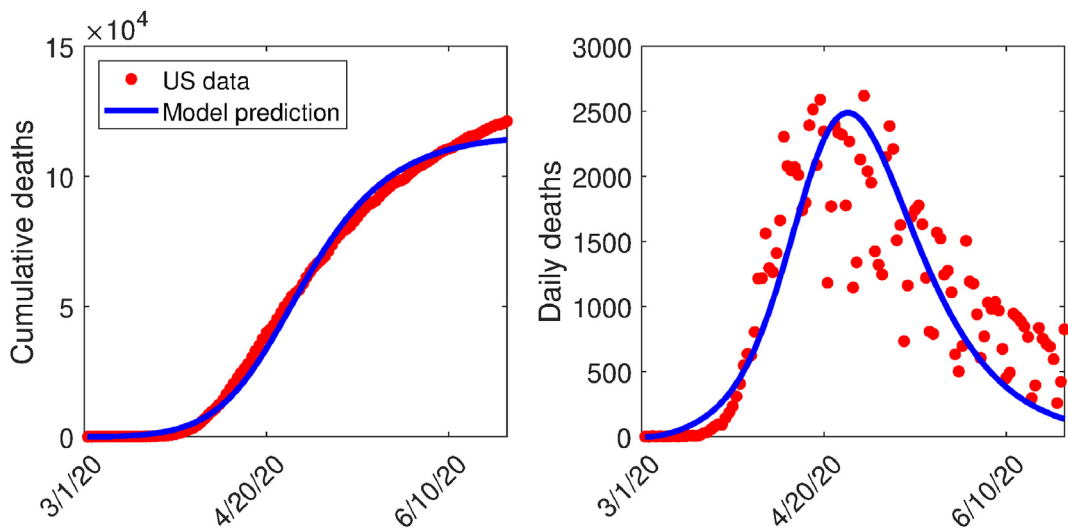


Fig. 2. (a) Data fitting of the model (2.1) in the absence of vaccination using COVID-19 mortality data for the US (Centers for Disease Control and Prevention, 2019; World Health Organization, 2019). (b) Simulations of the model (2.1) (using the estimated parameters) illustrating the daily mortality curve. The red dots represent data points, while the solid blue line represent predictions of death from model (2.1) for the period between March 1, 2020 through June 23, 2020.

calibrate the six parameters, we used a nonlinear least squares method to determine the set of parameters that minimizes the sum of the squares of the differences between the cumulative death predictions of the vaccination-free version of the model (2.1) and the observed cumulative COVID-19 mortality. The result obtained is depicted in Fig. 2 (left panel). Furthermore, the observed daily deaths are plotted alongside the predicted daily deaths generated using the vaccination-free version of the model (2.1) with the parameter values obtained from the fitting of the cumulative cases (right panel of Fig. 2). The values of the calibrated parameters obtained are tabulated in Table 3(b). Since no vaccine-related data for COVID-19 are currently available, we assumed that the hypothetical vaccine considered in this study has a baseline protective efficacy of 80% (i.e., we set $\epsilon_v = 0.8$). Further, we assume the baseline value of the vaccination rate (ξ_v) is 0.0203 per day.

It is noteworthy from the fitted parameters in Table 3 (b) that the sum of the fitted values of the community contact rates for the pre-symptomatic (β_e) and asymptotically-infectious individuals (β_a) overwhelmingly exceeds that for the symptomatically-infectious individuals (β_s). Thus, our fitting suggests that pre-symptomatic and asymptomatic infectious individuals are the overwhelming drivers of the pandemic in the US. In other words, the vast majority of the COVID-19 infections in the US is caused by COVID-19-infected individuals who are unaware of their infection status (i.e., those in the E_2 and I_a classes). Tindale et al. (Tindale et al., 2020) also showed that pre-symptomatic transmission played a significant role in COVID-19 dynamics in Singapore (accounting for 40-50% of transmissions) and Tianjin, China (60-80% of transmissions).

3.3. Vaccine-induced herd immunity threshold

For vaccine-preventable diseases, not all susceptible individuals can be immunized for various reasons, such as they are too young to be vaccinated (vaccinating infants or young children can, sometimes, harm the infants/children), they have co-morbidities and weakened immune system (and vaccinating may make their prognosis worse), they are of advanced age or they opt out for cultural, traditional or religious reasons. The question then is what is the minimum proportion of those we can vaccinate that we need to vaccinate so that those that we cannot vaccinate can be protected from developing severe disease or dying of the disease. The notion of *herd immunity* in the transmission dynamics is associated with the indirect protection, against acquisition of a communicable disease, members of the community receive when a large percentage of the population has become immune to the infectious disease due to natural recovery from prior infection or vaccination (Anderson, 1992; Anderson & May 1985). The consequence of herd immunity is that individuals who are not immune (e.g., those who cannot be vaccinated or those who have not been infected yet) receive some protection against the acquisition of the disease. The safest and fastest way to achieve herd immunity is obviously vaccination. It should, however, be mentioned that Sweden employed the other mechanism for achieving herd immunity in the context of COVID-19 dynamics in Sweden (Friedman, 2020). In other words, the Swedish public health agencies aimed to build herd immunity by not implementing the basic community transmission reduction strategies (e.g., social distancing, community lockdowns, use of face masks in public, contact tracing etc.) implemented in almost every country or community that is hard-hit with the COVID-19 pandemic, opting, instead, to allow individuals to acquire infection and, hopefully, recover from it. Although some level of this *natural herd immunity* has been achieved in Sweden, the COVID-

induced mortality recorded in Sweden far exceed those recorded for neighbouring Scandinavian countries that implemented the aforementioned non-pharmaceutical interventions (Friedman, 2020).

In this section, a theoretical condition for achieving community-wide vaccine-induced herd immunity is derived. Let $f_v = \frac{S_v^*}{N^*}$ be the fraction of unvaccinated susceptible individuals that have been vaccinated at the disease-free steady-state. It follows that the control reproduction number (\mathcal{R}_c) can then be re-written, in terms of f_v , as follows:

$$\mathcal{R}_c = \mathcal{R}_0(1 - \varepsilon_M c_M) \left[\frac{S_u^* + (1 - \varepsilon_v)S_v^*}{N^*} \right], \quad (3.5)$$

which can be simplified as (for the special case with \mathcal{R}^* being infinitesimally small in comparison to the total initial population $N(0)$)

$$\mathcal{R}_c \approx \mathcal{R}_0(1 - \varepsilon_M c_M)(1 - \varepsilon_v f_v). \quad (3.6)$$

Setting $\mathcal{R}_c = 1$ in (3.6), and solving for f_v , gives the following vaccine-induced herd immunity threshold for the model (2.1):

$$f_v \approx \frac{1}{\varepsilon_v} \left[1 - \frac{1}{\mathcal{R}_0(1 - \varepsilon_M c_M)} \right] = f_v^c, \quad \text{with } \varepsilon_M c_M \neq 1. \quad (3.7)$$

It follows from (3.6) and (3.7) that $\mathcal{R}_c < (>) 1$ whenever $f_v > (<) f_v^c$. This implies that if $f_v > f_v^c$, then the epidemic dies out (in line with Theorems 3.1 and 3.2). Furthermore, if $f_v < f_v^c$, then the epidemic rises, reaches a peak, and eventually declines to zero (in line with Theorem 3.1).

In order to obtain the projected value of the vaccine-derived community herd immunity threshold for the US, we compute the value of basic reproduction number (\mathcal{R}_0), from Equation (3.3) and using the baseline values of the community contact rates (β_e , β_a and β_s) and other parameters in Table 2. This gives $\mathcal{R}_0 = 3.16$. Substituting this value of \mathcal{R}_0 into (3.7), and noting that the vaccine efficacy is assumed to be 80% (i.e., $\varepsilon_v = 0.8$) and the baseline values of face masks efficacy and compliance given in Table 3 (i.e., $\varepsilon_M = 0.5$ and $c_M = 0.1704$, respectively), shows that the vaccine-derived community herd immunity threshold for the US is approximately 82% (see Table 4). The epidemiological implication of this result is that the pandemic can be effectively controlled (i.e., community transmission of COVID-19 can be significantly curtailed or the disease can be eliminated) if at least 82% of the susceptible US population is vaccinated.

The aforementioned required vaccine coverage herd immunity percentage is certainly on the high side, and may not be realistically attainable. In fact, Dr. Anthony Fauci, a member of the US Presidential Task Force on COVID-19, stated on June 29, 2020 that the hypothetical anti-COVID-19 vaccine may not reach the required high immunity in the US if many people refuse to get it (Cable News Network, 2020). One way to get around this need for high vaccine coverage to achieve high immunity is to combine the vaccination program with another anti-COVID-19 intervention, such as the use of face masks in public. Table 4 shows that the required herd immunity threshold decreased to (perhaps a more realistically-attainable) 72% if half the US population wears face masks in public. Further, only 46% of the US population would need to be vaccinated if everyone wears face mask in public. Thus, these simulations show that combining the vaccination program (using the hypothetical anti-COVID-19 vaccine with assumed efficacy of 80%) with a public face mask use strategy significantly enhances the prospect of COVID-19 elimination in the US.

Fig. 3 depicts the cumulative mortality as a function of time for various values of the steady-state vaccination coverage (f_v). This figure shows an increase in the cumulative mortality when $f_v < f_v^c$ and a decrease when $f_v > f_v^c$ (it should be mentioned that this figure was generated for the case where the vaccination program is implemented on March 1, 2020; this explains why the cumulative mortality numbers generated from the model are much lower than the mortality numbers actually recorded in the US over the same time period). It is worth mentioning that our results for the herd immunity threshold are subject to the homogeneous mixing assumption made in the formulation of the model (2.1). It is quite possible that the required herd immunity threshold for the US may change (i.e., be lower than what we estimated) if the homogeneous mixing assumption is relaxed (i.e., if heterogeneities in mixing, perhaps based on age or socio-economic status, is incorporated into the model).

4. Numerical simulations of vaccine impact

The model (2.1) is now simulated to assess the population-level impact of the hypothetical imperfect anti-COVID-19 vaccine in the US. The population-level impact of the vaccination rate (ξ_v) on the burden of the pandemic is monitored first of all. In these simulations, the public face mask use strategy is not implemented. The model (2.1) is then simulated using

Table 4

Community herd immunity threshold (f_v) for the US for various levels of mask compliance (c_M). Parameter values used are as given in Table 3.

Mask compliance percentage (c_M)	0%	10%	17.04% (baseline)	30%	50%	100%
Herd immunity threshold (f_v)	85.4%	83.4%	81.8%	78.5%	72.3%	45.9%

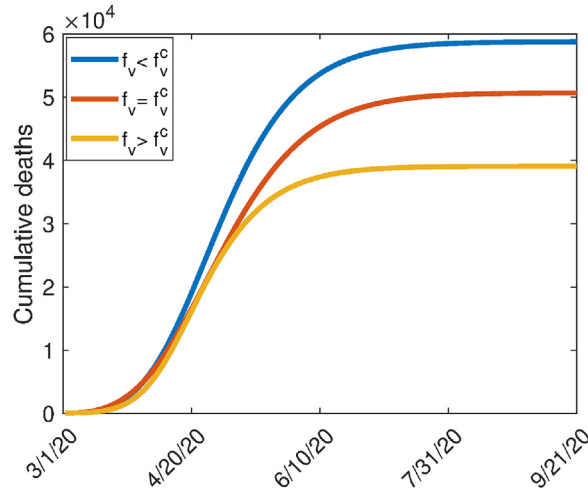


Fig. 3. Simulations of the model (2.1), showing the cumulative COVID-19 mortality as a function of time for various levels of herd immunity threshold (f_v). (a) $f_v < f_v^c$ ($r = 0.2$) (b) $f_v = f_v^c$ ($r = 0.35$) (c) $f_v > f_v^c$ ($r = 0.7$). Other parameter values used are as given in Table 3. For these simulations, the vaccination program is assumed to be implemented at the onset of the pandemic (starting March 1, 2020).

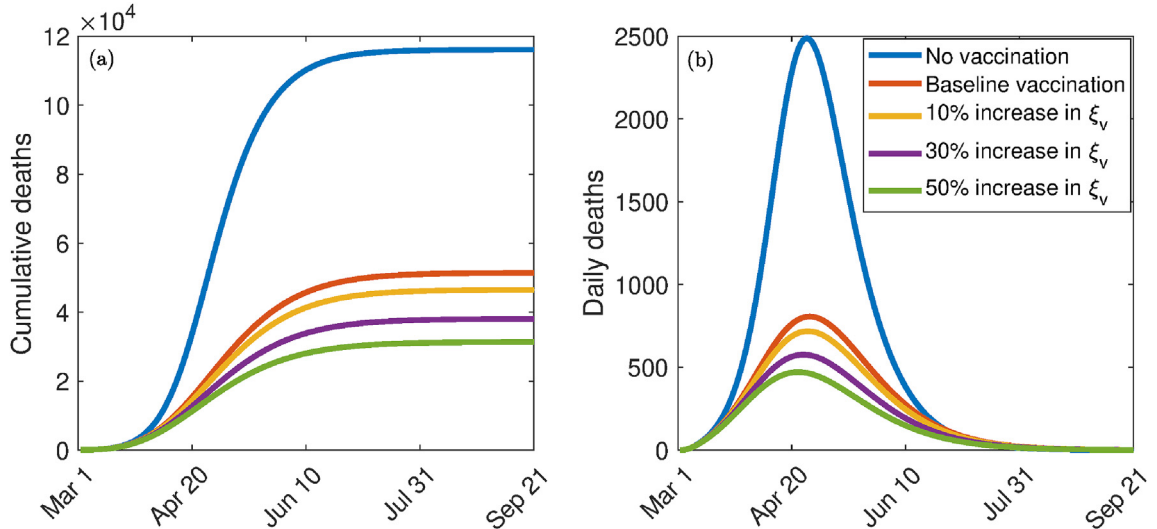


Fig. 4. Effect of vaccination coverage. Simulations of the model (2.1) showing the effect of the vaccination rate (ξ_v) on COVID-19 burden measure in terms of (a) cumulative deaths and (b) daily deaths. Parameter values used are as given in Table 3, with $c_M = \varepsilon_M = 0$ and various values of ξ_v .

the baseline parameter values in Table 3 (with $c_M = \varepsilon_M = 0$) and various values of ξ_v . The results obtained, depicted in Fig. 4, show that, for the worst-case scenario without vaccination and face masks usage in public (i.e., the model (2.1) with $\xi_v = S_v = \varepsilon_M = c_M = 0$), the US could record up to 110,000 cumulative deaths at the pandemic peak Fig. 4(a). The corresponding projected daily mortality is 2400 Fig. 4(b). These simulations show a dramatic reduction in the cumulative and the daily COVID-induced mortality (in comparison to the worst-case scenario without vaccination and mask usage) with increasing values of the vaccination rate ξ_v (from its baseline value). In particular, a 10% increase in the baseline value of ξ_v for the US resulted in a decrease in the cumulative number of deaths at the pandemic peak from 120,000 to 46,000 (Fig. 4 (a)). Furthermore, this corresponds to a decrease in the projected daily mortality from 2400 to 700, representing a 71% reduction (Fig. 4 (b)). Similarly, a 30% increase in the baseline value of ξ_v resulted in a marked reduction of the daily deaths at the pandemic peak to 580 (corresponding to a decrease in the projected cumulative mortality from 120,000 to 25,000). Thus, these simulations suggest that a significantly large increase in vaccination rate (from baseline) is necessarily needed to eliminate COVID-19 in the US using the hypothetical vaccine.

The model (2.1) is simulated to allow for the assessment of the impact of social distancing measures (aimed at reducing community transmission) with the implementation of vaccination and public mask usage in the community. We consider

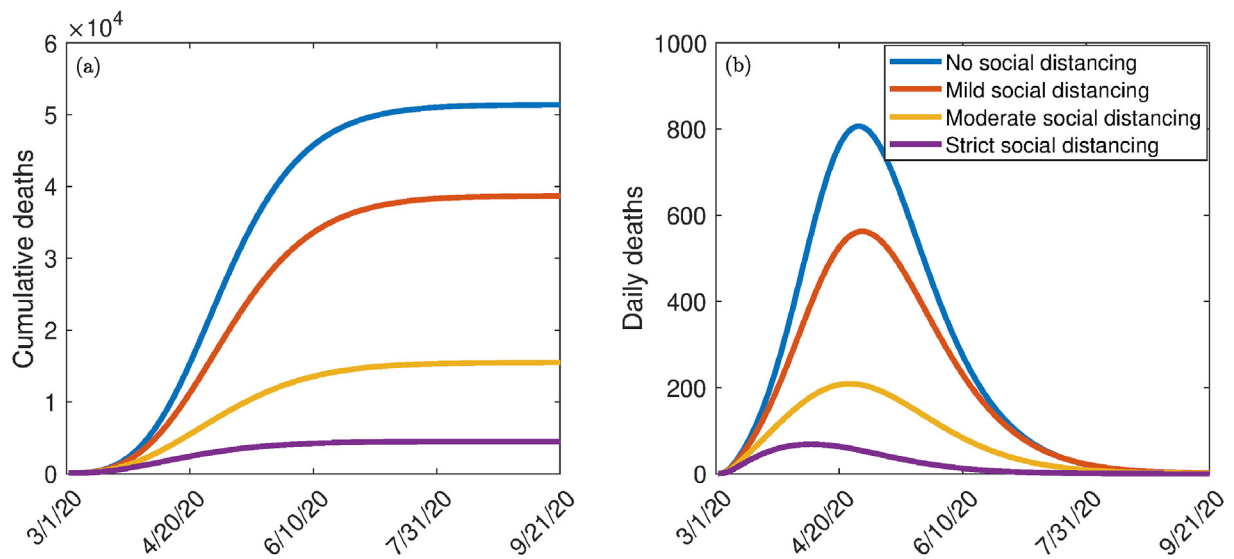


Fig. 5. Simulations of the model (2.1) for the impact of various effectiveness of social distancing control measures in the presence of vaccination on (a) cumulative deaths, (b) daily deaths. Mild, moderate, and strict (high) social distancing corresponds to 10%, 30%, and 50%, decrease in the values of the community contact rates β_e , β_a , and β_s from their baseline values, respectively. Parameter values used are as given in Table 3.

three levels of social distancing effectiveness, namely mild, moderate and high (strict). We model these effectiveness levels in terms of reduction in the community contact rate parameters (β_e , β_a and β_s), in comparison to their baseline values. In particular, we set mild, moderate, and strict (high) social distancing to correspond to a 10%, 30%, and 50% reduction, respectively, in the values of the contact rate parameters, in relation to their baseline values in Table 3. The simulation results obtained, depicted in Fig. 5, shows a marked decrease in disease burden (measured in terms of daily and cumulative COVID-induced mortality) with increasing effectiveness of social distancing, as expected. For instance, while Fig. 5 shows that up to 51,000 cumulative mortality can be recorded if social distancing measures were not implemented, the cumulative mortality dramatically decreases to about 5000 (representing about 90% reduction in cumulative mortality) if strict social distancing measures were implemented (Fig. 5 (a)). Similarly, Fig. 5 shows that up to 810 daily mortality can be recorded in the US if social distancing measures were not implemented, the daily mortality dramatically decreases to about 70 (representing about 91% reduction in daily mortality) if strict social distancing measures were implemented (Fig. 5 (b)). Thus, these simulations suggest that the implementation of the vaccination program alongside mask use and social distancing is more effective than if only the first two strategies are used.

Simulations were also carried out to assess the impact of vaccine efficacy and coverage on this disease dynamics. This is done for the special case of the model in the absence of the use of masks in the public (i.e., the model (2.1) with $c_M = \varepsilon_M = 0$). Specifically, a contour plot of the control reproduction number (\mathcal{R}_c) of the model, as a function of coverage (f_v) and vaccine efficacy (ε_v), is depicted in Fig. 6. This figure shows a decrease in the value of the reproduction number with increasing coverage and efficacy of the vaccine, as expected. For the assumed 80% efficacy of the hypothetical vaccine (i.e., $\varepsilon_v = 0.8$) in Table 3 (a), the simulations depicted in Fig. 6 show that nationwide elimination of COVID-19 can be achieved (i.e., \mathcal{R}_0^* can be brought to a value below unity) if at least 85.4% of the US populace is vaccinated.

The effect of the combined implementation of vaccination and social distancing strategies, on the control reproduction number (\mathcal{R}_c) of the model (2.1), is also monitored, by generating contour plots of \mathcal{R}_c , as a function of vaccination coverage (f_v) and efficacy (ε_v), for the aforementioned three levels (low, moderate and high) of social distancing effectiveness. The results obtained, depicted in Fig. 7, show that COVID-19 elimination (measured in terms of bringing \mathcal{R}_c to a value less than unity) is feasible even if social distancing is implemented at a low (mild) level of effectiveness (left panels of Fig. 7). In particular, Fig. 7 (a) shows that, with the assumed 80% efficacy of the vaccine, the implementation of social distancing at low effectiveness level will lead to the elimination of COVID-19 if the vaccine coverage is at least 81%. This required coverage decreases with increasing effectiveness of the social distancing measures (Fig. 7 (b) and (c)).

Additional numerical simulations were carried out to assess the community-wide impact of the combined impact of vaccination with a public face mask use strategy (as measured in terms of reduction in the value of control reproduction number, \mathcal{R}_c). The results obtained, depicted in Fig. 8, show a decrease in \mathcal{R}_c with increasing vaccine efficacy and compliance. For the fixed vaccine efficacy at 80%, our results show that if 10% of the US population wear face masks in public, the minimum vaccine coverage needed to eliminate the disease is approximately 83%. The minimum coverage needed to eliminate the pandemic decreases to 79% and 72%, respectively, if 30% and 50% of the US population wear face masks in public (Fig. 8 (a), (b) and (c)). Thus, the simulations in Figs. 7 and 8 also emphasize the fact that the prospect of

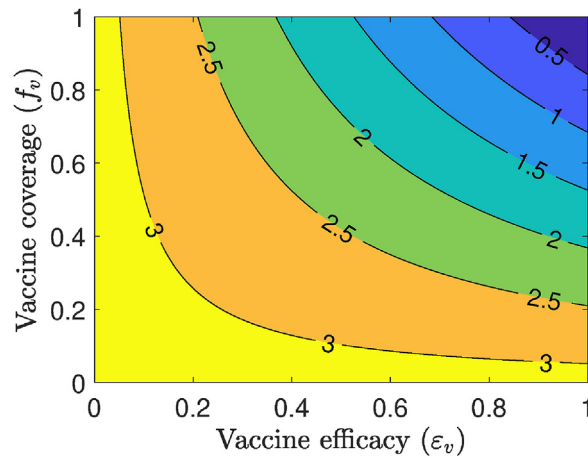


Fig. 6. Effects of vaccination as the only intervention strategy. Contour plots of the control reproduction number (\mathcal{R}_c) of the model (2.1), as a function of vaccine coverage (f_v) and vaccine efficacy (ε_v), for the baseline scenarios in Table 3 and in the absence of mask usage in public for the US. Parameter values used are as given in Table 3 with $\varepsilon_M = c_M = 0$.

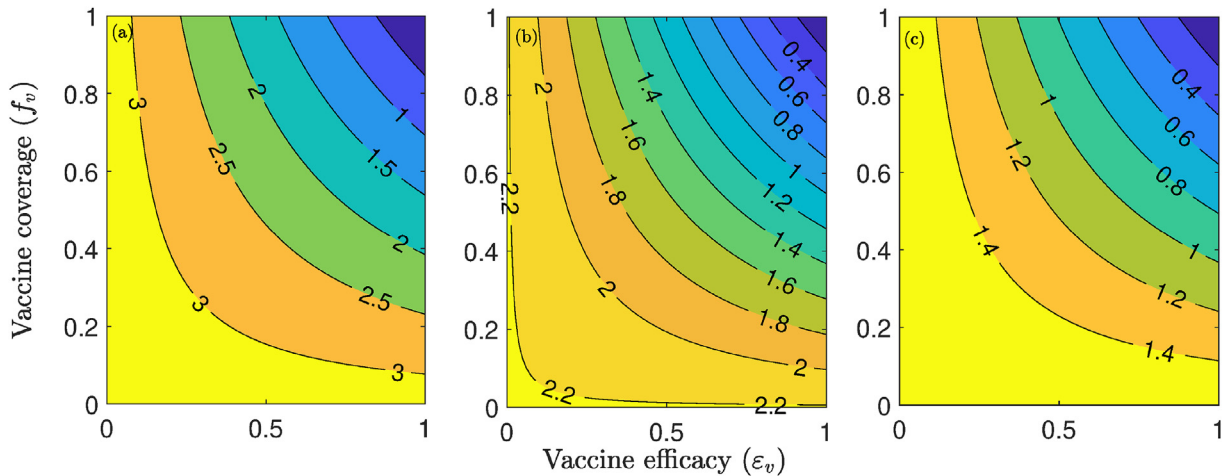


Fig. 7. Effect of combined vaccination and social distancing strategies. Contour plots of the control reproduction number (\mathcal{R}_c), as a function of vaccine coverage (f_v) and vaccine efficacy (ε_v) for the special case of the model (2.1) with no mask use in public. (a) mild social distancing (i.e., 10% decrease in β_e , β_s and β_a). (b) Moderate social distancing (i.e., 30% decrease in β_e , β_s and β_a). (c) Strict social distancing (i.e., 50% decrease in β_e , β_s and β_a). Parameter values used are as given in Table 3.

COVID-19 elimination using a vaccine is greatly enhanced if the vaccination program is complemented with another anti-COVID-19 intervention (such as face masks usage in public and social distancing), particularly if the complementary intervention is implemented at moderate or high effectiveness level (i.e., implemented universally, and with high efficacy and compliance).

5. Discussion and conclusions

A novel Coronavirus (COVID-19) emerged in China in December 2019. The virus, which is caused by SARS-CoV-2, rapidly spread to over 210 countries causing over 10 million confirmed cases and 500,000 deaths globally (as of June 28, 2020). Although there are currently no safe and effective vaccine for use in humans, numerous concerted global efforts are underway aimed at developing such vaccine. In fact, a number of candidate vaccines are undergoing advanced stages of clinical trials. One of the most promising of these efforts is the candidate vaccine being developed by a research group at Oxford University, which is expected to be available as early as January 2021 (or, latest, by the spring of 2021). We developed a mathematical model for assessing the potential community-wide impact of a hypothetical imperfect vaccine against the COVID-19 pandemic in the US. The model we developed, which takes the form of a deterministic system of nonlinear differential

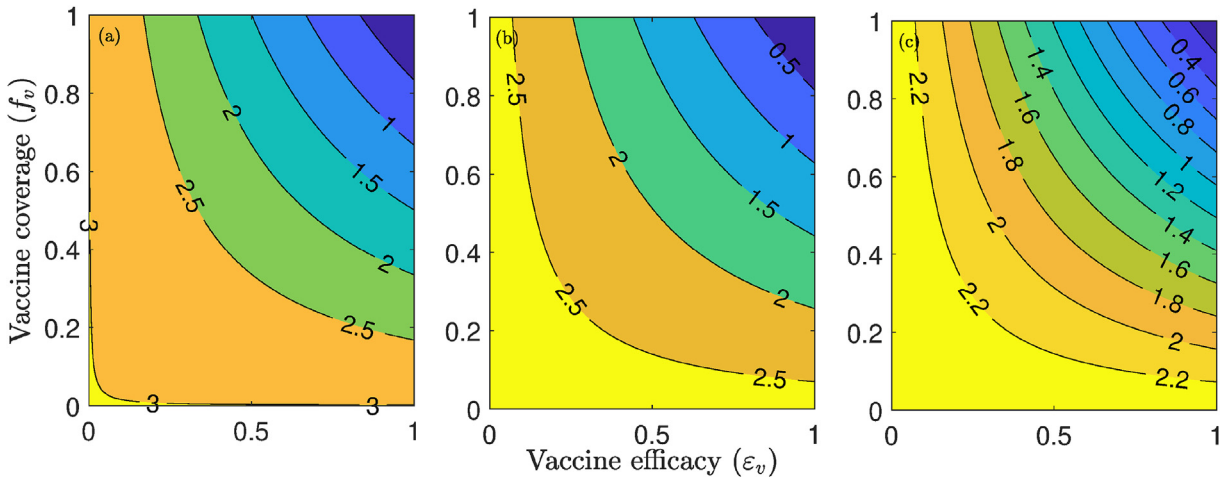


Fig. 8. Contour plots of the control reproduction number (\mathcal{R}_c), as a function of vaccine coverage (f_v) and vaccine efficacy (ε_v) for (a) 10% mask compliance, (b) 30% mask compliance, and (c) 50% mask compliance. Parameter values used are as given in Table 3 with various values of c_M .

equations, was parametrized using COVID-19 data for the US. The hypothetical vaccine was assumed to offer imperfect protective efficacy against the acquisition of COVID-19 infection.

The model was rigorously analysed to gain insight into its dynamical features. These analyses reveal that the continuum of disease-free equilibria of the epidemic model is asymptotically-stable whenever a certain epidemiological threshold, known as the control reproduction number (denoted by \mathcal{R}_c), is less than unity. The epidemiological implication of this result is that the community transmission of COVID-19 can be significantly curtailed if $\mathcal{R}_c < 1$. In other words, the routine vaccination against COVID-19 (using the hypothetical vaccine) can lead to the effective control or elimination of the pandemic if it can bring (and maintain) \mathcal{R}_c to a value less than unity. Furthermore, threshold quantities for the community vaccine-induced herd immunity were calculated. Our computations show, using the baseline values of the parameters of the model, that at least 82% of the US population needs to be vaccinated in order to achieve nationwide vaccine-derived herd immunity. This required vaccine coverage is certainly on the high side, and may not be easily attained for so many reasons, ranging from the expected insufficient stockpile of the vaccine during the early stages of their deployment, general apathy towards vaccination and the sizable percentage of people that cannot be vaccinated for medical, personal and other reasons (in fact, Dr. Anthony Fauci, a member of the US Presidential Task Force on COVID-19 warned on June 28, 2020 that the hypothetical vaccine may not generate the required level of herd immunity if too many people in the US decide not to be vaccinated (Cable News Network, 2020)). Our simulations showed that if the vaccination strategy is complemented with other public health interventions, such as a public mask use strategy for instance, the minimum herd immunity threshold required to effectively control the COVID-19 pandemic significantly reduces to a more realistically-attainable level. For example, if vaccination (using a vaccine with the assumed efficacy of 80%) is combined with a public face mask strategy with 30% mask compliance nationwide, the herd immunity threshold for the entire US decreases to 79%. In fact, this threshold decreases to only 46% if everyone in the US (who can wear a face mask) wears face mask in public. Thus, this study shows that the prospect of the effective control of COVID-19 using routine vaccination (with the hypothetical vaccine) is significantly enhanced if the vaccination program is combined with a public face mask use strategy (especially if the effectiveness and coverage of the face mask use strategy are high enough).

We also carried out numerical simulations to measure the population-level impact of the rate at which the hypothetical vaccination is administered. The results obtained showed that the COVID-19 burden (as measured in terms of daily and cumulative COVID-induced mortality) decreases with increasing vaccination rate, as expected. Our simulations showed that high increases in the vaccination rate (from its baseline value) is necessarily needed to achieve significant reduction in disease burden. We also simulated the combined effect of implementing the routine vaccination program with social distancing (in the absence of face mask usage). We showed that COVID-19 can be effectively controlled using the two interventions even if the effectiveness level of social distancing is low (as long as the vaccine coverage is high). In particular, our simulations showed that the control reproduction number (\mathcal{R}_c) can be reduced to a value less than unity (needed for the effective control of the disease, in line with the local and global asymptotic stability property of the continuum of disease-free equilibria, established in Section 3).

We assessed the population-level impact of combining the routine vaccination strategy with a public mask use strategy. Our simulations show a decrease in the burden of the COVID-19 pandemic (again as measured in terms of reduction in the value of the reproduction number \mathcal{R}_c) with increasing efficacies and compliance of the vaccine and mask usage. It was shown that if the vaccine efficacy is fixed at the assumed 80% and mask compliance is fixed at the low value of 10%, COVID-19 can be eliminated if the vaccine coverage is at least 83%. The vaccine coverage decreases to 79%, 72%, and 46%, respectively, if mask

use compliance is increased to 30%, 50%, and 100%. Again, these result confirmed that COVID-19 elimination is more feasible if the vaccination program is combined with another intervention (face mask use in public, in this case).

In summary, this study shows that the prospect of eliminating COVID-19 in the US using the imperfect hypothetical vaccine is promising. This prospect is greatly enhanced if the vaccination program is combined with other interventions that limit community transmission, such as social distancing and face mask use in public. Certain factors may affect the results we presented in this study. The first is that the absence of vaccine-related data forced us to make assumptions on the expected efficacy of the hypothetical vaccine (ε_v), as well as the rate at which it will be administered in the US (ζ_v). In particular, we assumed a vaccine efficacy of 80%, which may be higher than the efficacy of the COVID-19 vaccine we end up having in the future. Second, the model we developed in this study is based on assuming a well-mixed population. This simplifying homogeneous-mixing assumption (needed for mathematical tractability) constitutes another limitation of the study (in particular, the value for the vaccine-derived herd immunity threshold we estimated may be lowered if mixing heterogeneities are incorporated into the model). The authors plan to address these heterogeneities in a future study.

Declaration of competing interest

None.

Acknowledgments

One of the authors (ABG) acknowledge the support, in part, of the Simons Foundation (Award #585022) and the National Science Foundation (Award #1917512). CNN acknowledges the support of the Simons Foundation (Award #627346). The authors are grateful to the two anonymous reviewers and the Handling Editor for the constructive comments. The authors are grateful to Dr. Elamin H. Elbasha (Merck Inc.) for the careful reading of the manuscript and for the valuable comments on the computation of the vaccine-derived herd immunity threshold.

Appendix A. Proof of Theorem 3.2

Proof. Consider the model (2.1) with $\mathcal{R}_c \leq 1$. Furthermore, consider the following linear Lyapunov function:

$$\mathcal{L} = g_1 E_1 + g_2 E_2 + g_3 I_s + g_4 I_a,$$

where,

$$g_1 = \gamma_a(\phi_s + \gamma_s + \delta_s), \quad g_2 = g_1, \quad g_3 = \gamma_a \beta_s (1 - \varepsilon_M c_M) \text{ and } g_4 = (\phi_s + \gamma_s + \delta_s) \beta_a (1 - \varepsilon_M c_M)$$

It follows that the Lyapunov derivative is given by:

$$\begin{aligned} \dot{\mathcal{L}} &= g_1 \dot{E}_1 + g_2 \dot{E}_2 + g_3 \dot{I}_s + g_4 \dot{I}_a, = g_1 [(\lambda_e + \lambda_s + \lambda_a) [S_u + (1 - \varepsilon_v) S_v] - \sigma_1 E_1] + g_2 [\sigma_1 E_1 - \sigma_2 E_2] \\ &\quad + g_3 [(1 - r) \sigma_2 E_2 - (\phi_s + \gamma_s + \delta_s) I_s] + g_4 [r \sigma_2 E_2 - \gamma_a I_a], = g_1 \left[\beta_e (1 - \varepsilon_M c_M) \frac{E_2}{N} (S_u + (1 - \varepsilon_v) S_v) \right] \\ &\quad - g_2 \sigma_2 E_2 + g_3 (1 - r) \sigma_2 E_2 + g_4 r \sigma_2 E_2 + g_1 \left[\beta_a (1 - \varepsilon_M c_M) \frac{I_a}{N} (S_u + (1 - \varepsilon_v) S_v) \right] - g_4 \gamma_a I_a + g_1 \left[\beta_s (1 - \varepsilon_M c_M) \frac{I_s}{N} (S_u + (1 - \varepsilon_v) S_v) \right] \\ &\quad - g_3 (\phi_s + \gamma_s + \delta_s) I_s, \end{aligned}$$

which can be simplified to,

$$\begin{aligned} \dot{\mathcal{L}} &= \gamma_a (\phi_s + \gamma_s + \delta_s) \left[\beta_s (1 - \varepsilon_M c_M) \frac{I_s}{N} (S_u + (1 - \varepsilon_v) S_v) \right] - \gamma_a \beta_s (1 - \varepsilon_M c_M) (\phi_s + \gamma_s + \delta_s) I_s \\ &\quad + \gamma_a (\phi_s + \gamma_s + \delta_s) \left[\beta_a (1 - \varepsilon_M c_M) \frac{I_a}{N} (S_u + (1 - \varepsilon_v) S_v) \right] - (\phi_s + \gamma_s + \delta_s) \beta_s (1 - \varepsilon_M c_M) \gamma_a I_a \\ &\quad + \gamma_a (\phi_s + \gamma_s + \delta_s) \sigma_2 \left\{ \frac{\beta_e (1 - \varepsilon_M c_M) [S_u + (1 - \varepsilon_v) S_v]}{\sigma_2 N} + \frac{(1 - r) \beta_s (1 - \varepsilon_M c_M)}{(\phi_s + \gamma_s + \delta_s)} + \frac{r \beta_a (1 - \varepsilon_M c_M)}{\gamma_a} - 1 \right\} E_2, \end{aligned}$$

so that (noting that since $S_u(0) + S_v(0) \leq N(0)$ in Ω and $0 \leq \varepsilon \leq 1$, then $S_u(t) + (1 - \varepsilon_v) S_v(t) \leq N(t)$ for all t),

$$\dot{\mathcal{L}} \leq \gamma_a(\varphi_s + \gamma_s + \delta_s)\sigma_2 \left\{ \frac{\beta_e(1 - \varepsilon_M c_M)}{\sigma_2} + \frac{(1 - r)\beta_s(1 - \varepsilon_M c_M)}{(\varphi_s + \gamma_s + \delta_s)} + \frac{r\beta_a(1 - \varepsilon_M c_M)}{\gamma_a} - 1 \right\} E_2, \leq \gamma_a(\varphi_s + \gamma_s + \delta_s)\sigma_2(\mathcal{R}_c - 1)E_2.$$

Hence, $\dot{\mathcal{L}} \leq 0$ if $\mathcal{R}_c \leq 1$, and $\dot{\mathcal{L}} = 0$ if and only if $E_2(t) = 0$. Therefore, \mathcal{L} is a Lyapunov function for system (2.1). Substituting $E_2(t) = 0$ in the model (2.1) shows that $(S_u(t), S_v(t), E_1(t), E_2(t), I_s(t), I_a(t), I_h(t), R(t)) \rightarrow (S_u^*, S_v^*, 0, 0, 0, 0, 0, R^*)$ as $t \rightarrow \infty$. Furthermore, it can be shown that the largest compact invariant set in $\{(S_u(t), S_v(t), E_1(t), E_2(t), I_s(t), I_a(t), I_h(t), R(t)) \in \Omega : \dot{\mathcal{L}} = 0\}$ is the continuum of disease-free equilibria (\mathcal{E}_0). Hence, it follows, by the LaSalle's Invariance Principle, that the continuum of disease-free equilibria of the model (2.1) is a stable global attractor in Ω whenever $\mathcal{R}_c \leq 1$.

References

Anderson, R. M. (1992). The concept of herd immunity and the design of community-based immunization programmes. *Vaccine*, 10, 928–935.

Anderson, R. M., & May, R. M. (1985). Vaccination and herd immunity to infectious diseases. *Nature*, 318, 323–329.

Cable News Network, "Fauci says covid-19 vaccine may not get us to herd immunity if too many people refuse to get it," CNN (Assessed on June 29, 2020). (Online Version).

E. Callaway, "Scores of coronavirus vaccines are in competition — how will scientists choose the best?" A Nature research Journal (Assessed on April 30, 2020).

Center for Systems Science and Engineering at Johns Hopkins University. *COVID-19*. (2020). JHU CSSE (Online Version).

Centers for Disease Control and Prevention, "Coronavirus disease 2019 (COVID-19)," National Center for Immunization and Respiratory Diseases (NCIRD), Division of Viral Diseases (Accessed on March 4, 2020). (Online Version).

Center for Disease Control and Prevention. (June 6, 2020). *Covid-19 pandemic planning scenarios*. National Center for Immunization and Respiratory Diseases (NCIRD), Division of Viral Diseases (Online Version).

Davies, A., Thompson, K.-A., Giri, K., Kafatos, G., Walker, J., & Bennett, A. (2013). Testing the efficacy of homemade masks: Would they protect in an influenza pandemic? *Disaster Medicine and Public Health Preparedness*, 7, 413–418.

Diekmann, O., Heesterbeek, J. A. P., & Metz, J. A. (1990). On the definition and the computation of the basic reproduction ratio R_0 in models for infectious diseases in heterogeneous populations. *Journal of Mathematical Biology*, 28, 365–382.

Dong, E., Du, H., & Gardner, L. (2020a). An interactive web-based dashboard to track COVID-19 in real time. *The Lancet Infectious Diseases*.

van den Driessche, P., & Watmough, J. (2002). Reproduction numbers and sub-threshold endemic equilibria for compartmental models of disease transmission. *Mathematical Biosciences*, 180, 29–48.

Dong, E., Du, H., & Gardner, L. (2020b). Coronavirus COVID-19 global cases by Johns Hopkins CSSE. *The Lancet Infectious Diseases*. Online Version.

Eikenberry, S. E., Muncuso, M., Iboi, E., Phan, T., Kostelich, E., Kuang, Y., & Gumel, A. B. (2020). To mask or not to mask: Modeling the potential for face mask use by the general public to curtail the covid-19 pandemic. *Infectious Disease Modeling*, 5, 293–308.

Ferguson, N. M., Laydon, D., Nedjati-Gilani, G., Imai, N., Ainslie, K., Baguelin, M., Bhatia, S., Boonyasiri, A., Cucunubá, Z., Cuomo-Dannenburg, G., et al. (2020). *Impact of non-pharmaceutical interventions (NPIs) to reduce COVID-19 mortality and healthcare demand*. London: Imperial College COVID-19 Response Team. March 16.

T. L. Friedman, "Is Sweden doing it right?" New York Times (Assessed on May 4, 2020). (Online Version).

Hellewell, J., Abbott, S., Gimma, A., Bosse, N. I., Jarvis, C. I., Russell, T. W., Munday, J. D., Kucharski, A. J., Edmunds, W. J., Sun, F., et al. (2020). Feasibility of controlling COVID-19 outbreaks by isolation of cases and contacts. *The Lancet Global Health*.

Holshue, M. L., DeBolt, C., Lindquist, S., Lofy, K. H., Wiesman, J., Bruce, H., Spitters, C., Ericson, K., Wilkerson, S., Tural, A., et al. (2020). "First case of 2019 novel coronavirus in the United States," New England. *Journal of Medicine*.

Kirkpatrick, D. (May 2, 2020). *In race for a coronavirus vaccine, an Oxford group leaps ahead*. New York Times. Online Version.

S. Knvul and T. Katie, "More coronavirus vaccines and treatments move toward human trials," New York Times (Accessed on May 2, 2020). (Online Version).

Kucharski, A. J., Russell, T. W., Diamond, C., Liu, Y., Edmunds, J., Funk, S., Eggo, R. M., Sun, F., Jit, M., Munday, J. D., et al. (2020). Early dynamics of transmission and control of COVID-19: A mathematical modelling study. *The Lancet Infectious Diseases*.

Li, Q., Guan, X., Wu, P., Wang, X., Zhou, L., Tong, Y., Ren, R., Leung, K. S., Lau, E. H., Wong, J. Y., et al. (2020). "Early transmission dynamics in Wuhan, China, of novel coronavirus-infected pneumonia. *New England Journal of Medicine*.

Matthews, S. (May 2, 2020). *U.S. Jobless rate may soar to 30%*. Bloomberg Report (Online Version).

Mizumoto, K., & Chowell, G. (2020). Transmission potential of the novel coronavirus (COVID-19) onboard the Diamond princess cruise ship, 2020. *Infectious Disease Modelling*.

Ngonghala, C. N., Iboi, E., Eikenberry, S., Scotch, M., MacIntyre, C. R., Bonds, M. H., & Gumel, A. B. (2020). Mathematical assessment of the impact of non-pharmaceutical interventions on curtailing the 2019 novel coronavirus. *Mathematical Biosciences*, 325, 108364.

Nishiura, H., & Chowell, G. (2009). The effective reproduction number as a prelude to statistical estimation of time-dependent epidemic trends. In *Mathematical and statistical estimation approaches in epidemiology* (pp. 103–121). Springer.

Rotman, D. (May 2, 2020). *Stop COVID or save the economy? We can do both*. MIT Technology Review (Online Version).

Tang, B., Wang, X., Li, Q., Bragazzi, N. L., Tang, S., Xiao, Y., & Wu, J. (2020). Estimation of the transmission risk of the 2019-ncov and its implication for public health interventions. *Journal of Clinical Medicine*, 9, 462.

Tindale, L. C., Stockdale, J. E., Coombe, M., Garlock, E. S., Lau, W. Y. V., Saraswat, M., Zhang, L., Chen, D., Wallinga, J., & Colijn, C. (2020). Evidence for transmission of covid-19 prior to symptom onset. *eLife*, 9, Article e57149.

World Health Organization, "Coronavirus disease (COVID-19) technical guidance," WHO (Accessed on March 4, 2020). Online Version.

World Health Organization, "reportCoronavirus disease (COVID-2019) situation reports," WHO (Accessed on March 19, 2020). Online Version.

World Health Organization. (2020b). *Coronavirus disease 2019 (COVID-19): Situation report (Vol. 46)*. WHO.

World Health Organization, "Emergencies, preparedness, response. Pneumonia of unknown origin – China," Disease Outbreak News (5 January, (Accessed on March 5, 2020). Online Version.

Zhou, F., Yu, T., Du, R., Fan, G., Liu, Y., Liu, Z., Xiang, J., Wang, Y., Song, B., Gu, X., et al. (2020). Clinical course and risk factors for mortality of adult inpatients with COVID-19 in wuhan, China: A retrospective cohort study. *The Lancet*.